

Cosmic Ray Anisotropy

Markus Ahlers

Niels Bohr Institute, Copenhagen

YITP Workshop

*“Connecting high-energy astroparticle physics
for origins of cosmic rays and future perspectives”*

December 7–10, 2020



The Niels Bohr
International Academy

VILLUM FONDEN



UNIVERSITY OF
COPENHAGEN

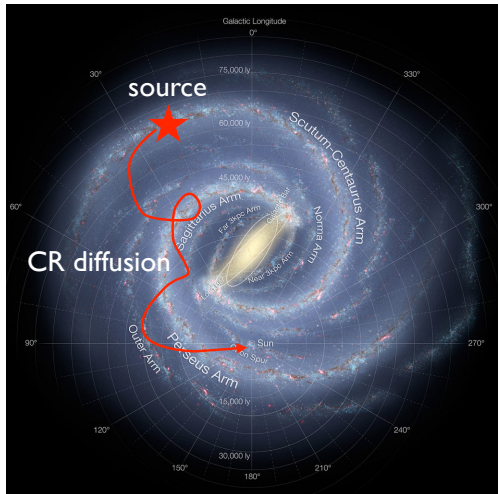


Galactic Cosmic Rays

- *Standard paradigm:*
Galactic CRs accelerated in
supernova remnants
- ✓ sufficient power: $\sim 10^{-3} \times M_{\odot}$
with a rate of ~ 3 SNe per century
[Baade & Zwicky'34]
- galactic CRs via diffusive shock
acceleration?
- energy-dependent **diffusion** through
Galaxy
- arrival direction **mostly isotropic**

$$n_{\text{CR}} \propto E^{-\gamma} \quad (\text{at source})$$

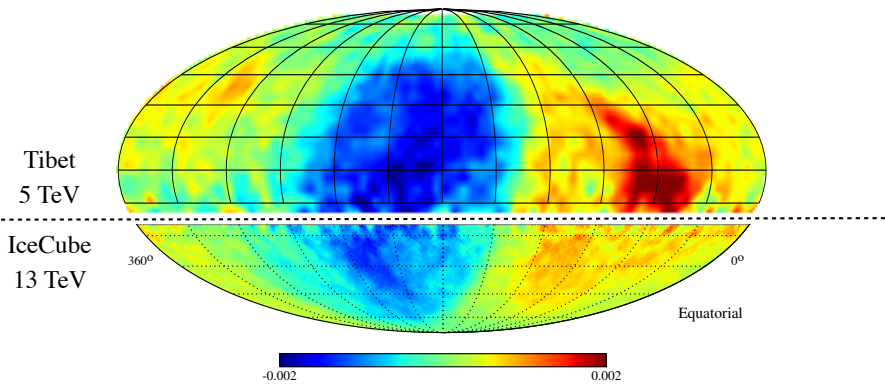
$$n_{\text{CR}} \propto E^{-\gamma-\delta} \quad (\text{observed})$$



Galactic Cosmic Ray Anisotropy

Cosmic ray anisotropies up to the level of **one-per-mille** at various energies
(Super-Kamiokande; Milagro; ARGO-YBJ; EAS-TOP, Tibet AS- γ ; IceCube; HAWC)

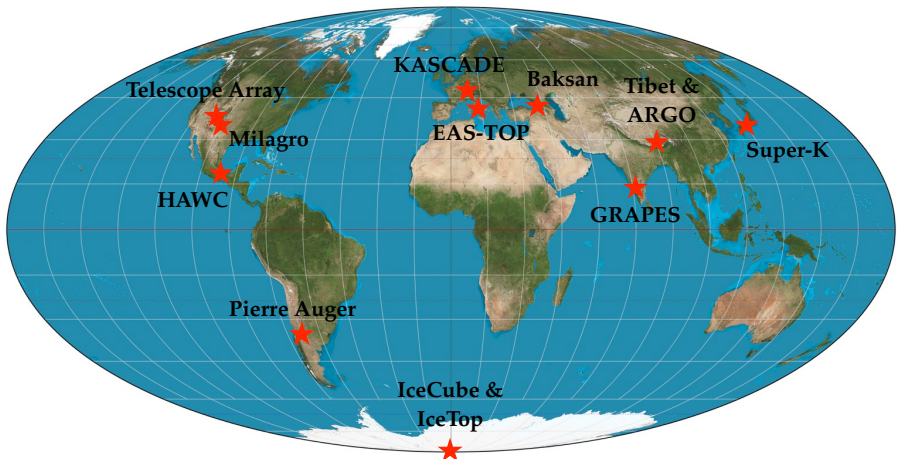
$$\text{Anisotropy} = \text{Relative Intensity} - 1$$



[e.g. review by MA & Mertsch'16]

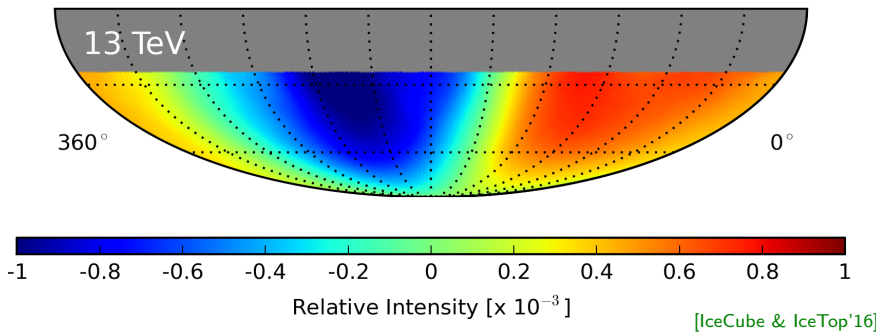
Galactic Cosmic Ray Anisotropy

Cosmic ray anisotropies up to the level of **one-per-mille** at various energies
(Super-Kamiokande; Milagro; ARGO-YBJ; EAS-TOP, Tibet AS- γ ; IceCube; HAWC)



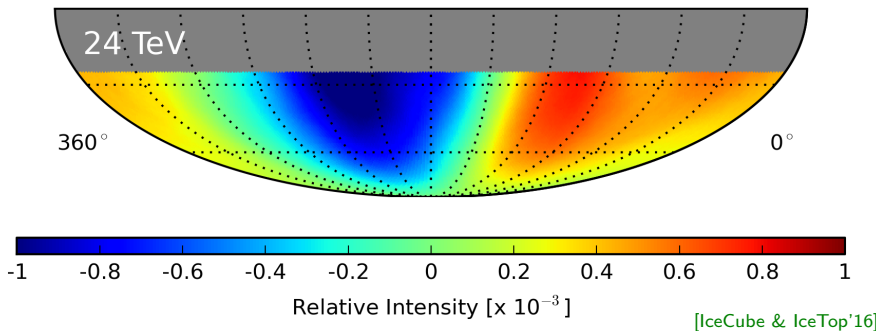
Energy-Dependence

Large-scale (dipole) anisotropy has strong energy dependence with phase-flip around 100 TeV.



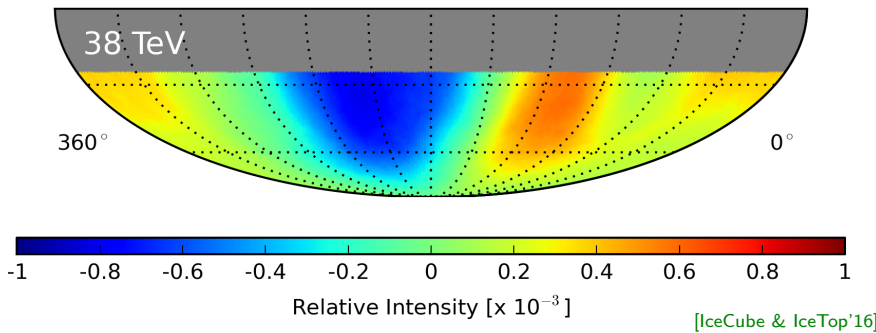
Energy-Dependence

Large-scale (dipole) anisotropy has strong energy dependence with phase-flip around 100 TeV.



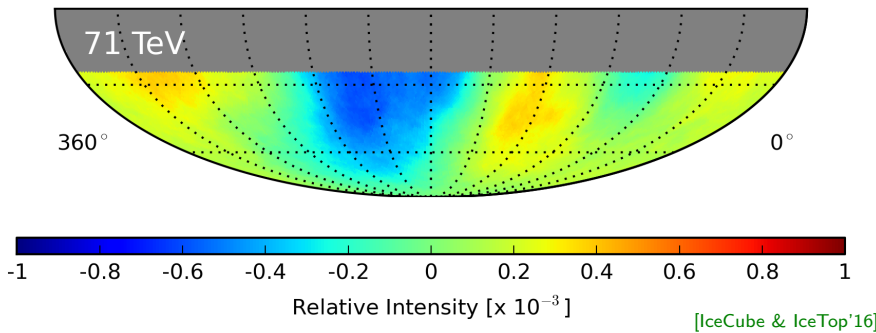
Energy-Dependence

Large-scale (dipole) anisotropy has strong energy dependence with phase-flip around 100 TeV.



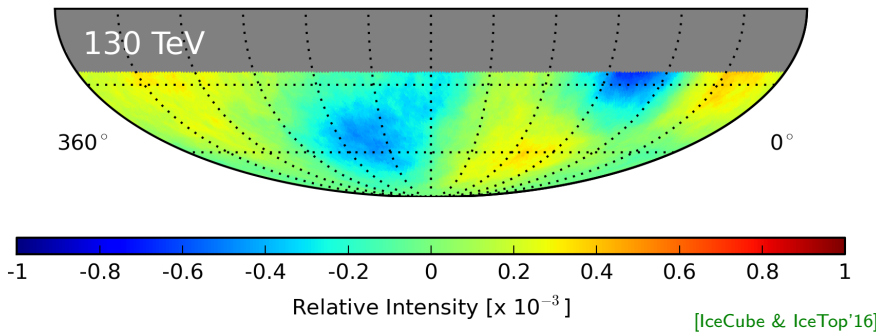
Energy-Dependence

Large-scale (dipole) anisotropy has strong energy dependence with phase-flip around 100 TeV.



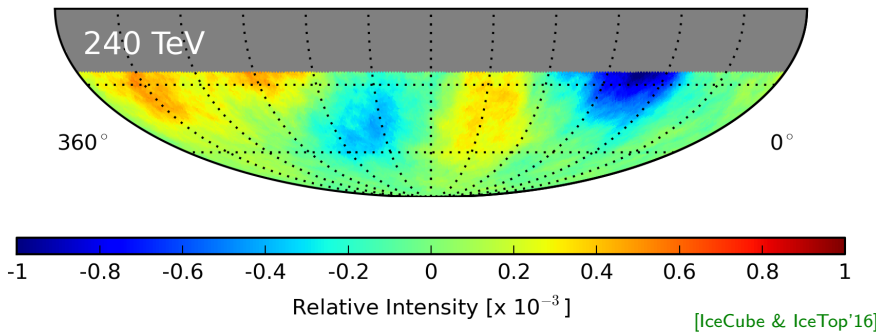
Energy-Dependence

Large-scale (dipole) anisotropy has strong energy dependence with phase-flip around 100 TeV.



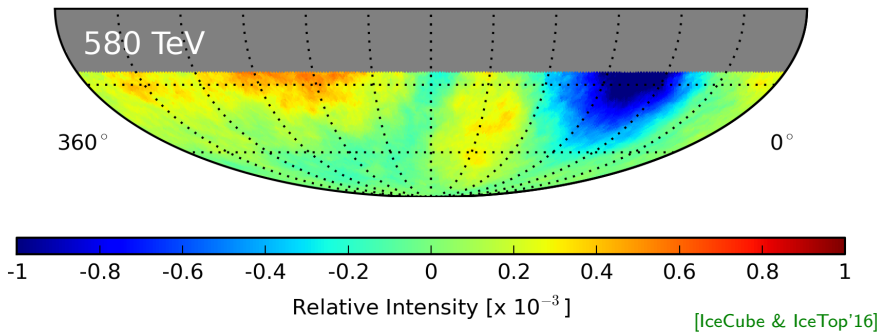
Energy-Dependence

Large-scale (dipole) anisotropy has strong energy dependence with phase-flip around 100 TeV.



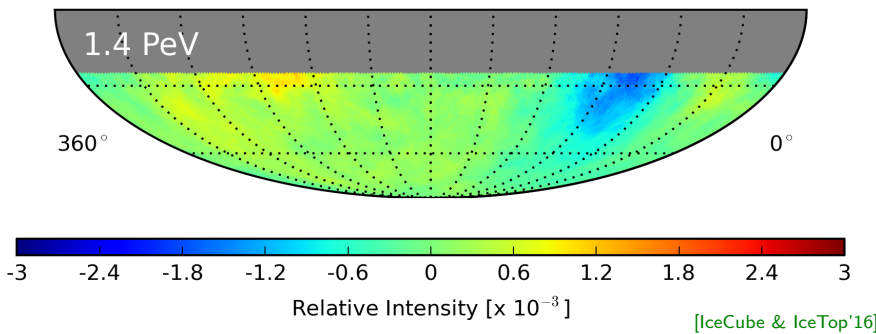
Energy-Dependence

Large-scale (dipole) anisotropy has strong energy dependence with phase-flip around 100 TeV.



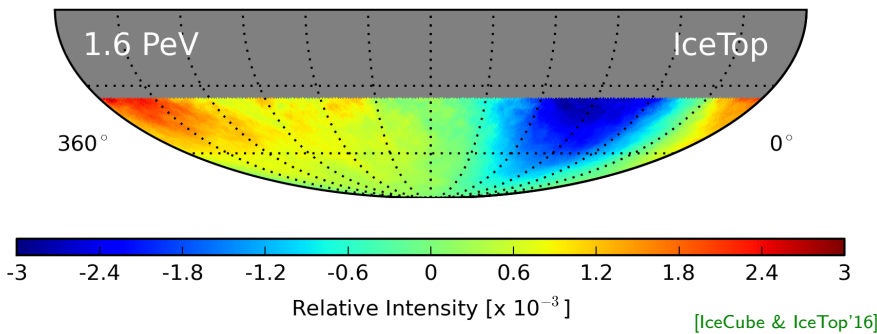
Energy-Dependence

Large-scale (dipole) anisotropy has strong energy dependence with phase-flip around 100 TeV.



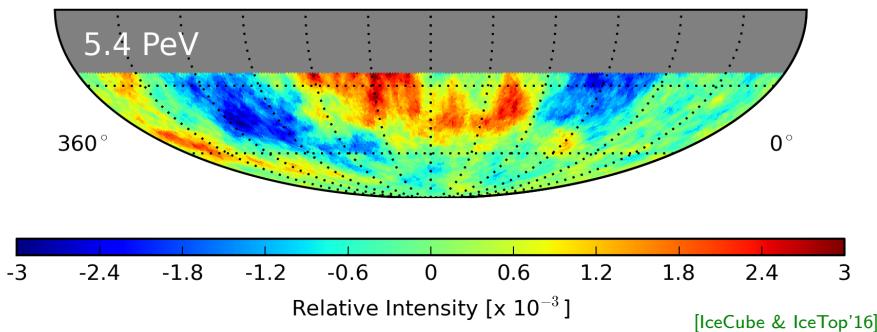
Energy-Dependence

Large-scale (dipole) anisotropy has strong energy dependence with phase-flip around 100 TeV.



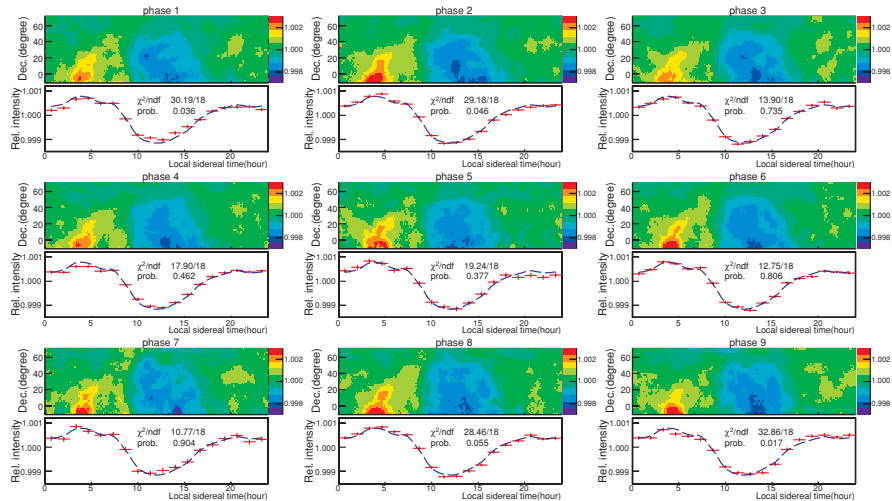
Energy-Dependence

Large-scale (dipole) anisotropy has strong energy dependence with phase-flip around 100 TeV.



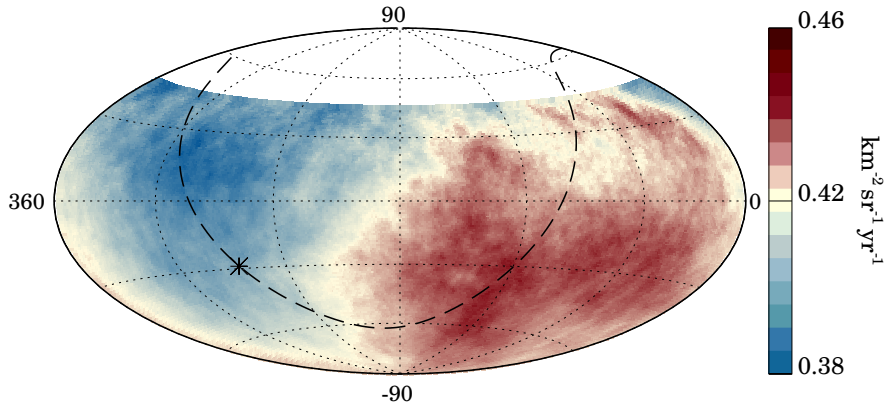
Time-Dependence

No significant variation of TeV-PeV anisotropy over time scales of $\mathcal{O}(10)$ years.



[Tibet-AS γ '10]

Recent Highlight: Auger Dipole Anisotropy



Energy [EeV]	Dipole component d_z	Dipole component d_{\perp}	Dipole amplitude d	Dipole declination δ_d [$^{\circ}$]	Dipole right ascension α_d [$^{\circ}$]
4 to 8	-0.024 ± 0.009	$0.006^{+0.007}_{-0.003}$	$0.025^{+0.010}_{-0.007}$	-75^{+17}_{-8}	80 ± 60
8	-0.026 ± 0.015	$0.060^{+0.011}_{-0.010}$	$0.065^{+0.013}_{-0.009}$	-24^{+12}_{-13}	100 ± 10

[Auger, Science'17]

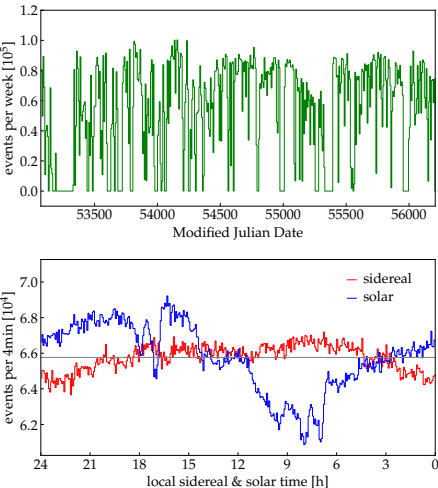
Anisotropy Reconstruction

Reconstruction Methods

- ✖ data is strongly **time-dependent**:
 - detector deployment/maintenance
 - atmospheric conditions
(day/night, seasons)
 - power outages,...

- ✖ local **anisotropies** of detector:
 - detector geometry
 - mountains
 - geo-magnetic fields,...

- two analysis strategies:
 - **Monte-Carlo & monitoring**
(limited by **systematic uncertainties**)
 - **data-driven likelihood methods**
(limited by **statistical uncertainties**)



example: KASCADE-Grande data

[MA'19]

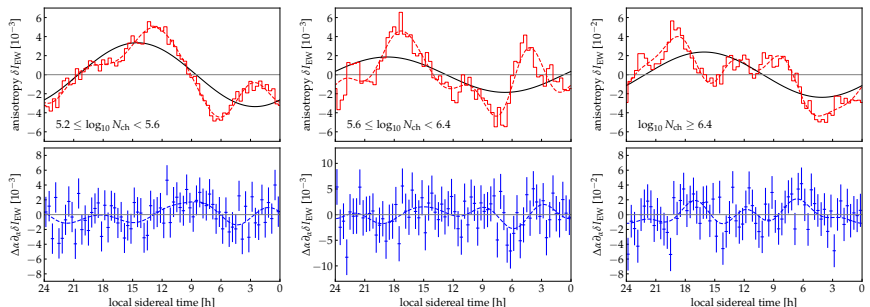
Data-Driven: East-West Method

- Strong time variation of cosmic ray background level can be compensated by differential methods.
- East-West asymmetry:**

[e.g. Bonino et al.'11]

$$A_{EW}(t) \equiv \frac{N_E(t) - N_W(t)}{N_E(t) + N_W(t)} \simeq \underbrace{\Delta\alpha \frac{\partial}{\partial\alpha} \delta I(\alpha, 0)}_{\text{if dipole!}} + \underbrace{\text{const}}_{\text{local asym.}}$$

- For instance, binned KASCADE-Grande data (2.7 PeV, 6.1 PeV & 33 PeV): [MA'19]



(no significant dipole anisotropy found)

Data-Driven: Likelihood Reconstructions

- ✗ East-West method introduces cross-talk between higher multipoles, regardless of field of view.
- ➔ Alternatively, data can be analyzed to *simultaneously* reconstruct:
 - **relative acceptance** $\mathcal{A}(\varphi, \theta)$ (in local coordinates)
 - **relative intensity** $I(\alpha, \delta)$ (in equatorial coordinates)
 - **background rate** $\mathcal{N}(t)$ (in sidereal time)
 - expected number of CRs observed in sidereal time bin τ and local coordinate i :

$$\mu_{\tau i} = \mu(\mathcal{I}_{\tau i}, \mathcal{N}_\tau, \mathcal{A}_i)$$

- reconstruction via maximum likelihood:

$$\mathcal{L}(n|I, \mathcal{N}, \mathcal{A}) = \prod_{\tau i} \frac{(\mu_{\tau i})^{n_{\tau i}} e^{-\mu_{\tau i}}}{n_{\tau i}!}$$

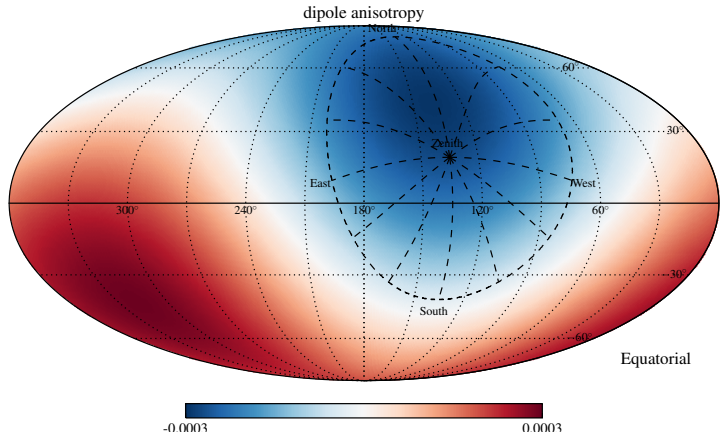
- Maximum can be reconstructed by iterative methods.

[MA et al.'15]

- ➔ used in joint IceCube & HAWC analysis

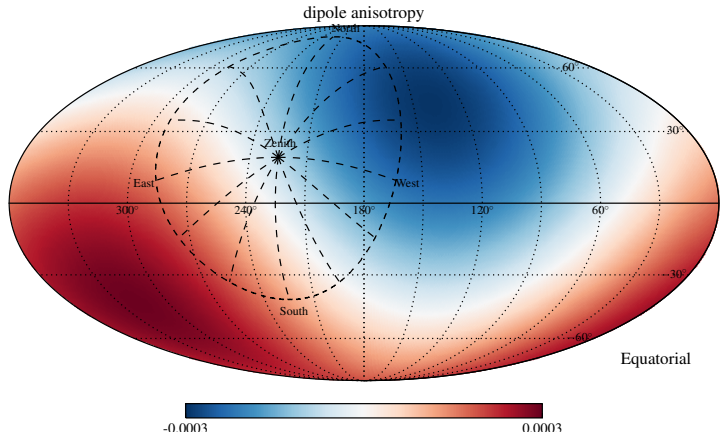
[IceCube & HAWC'18]

Issues with Data-Driven Reconstruction



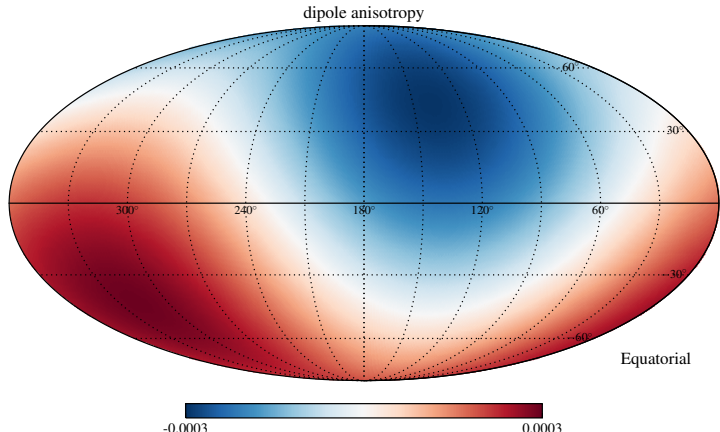
- ground-based detectors need to be **calibrated** by CR data
- true CR dipole defined by amplitude A_1 , and orientation $(\text{RA}, \text{DEC}) = (\alpha_1, \delta_1)$
- ✗ observable: projected dipole with amplitude $A'_1 = A_1 \cos \delta_1$ and orientation $(\alpha_1, 0)$
[Iuppa & Di Sciascio'13; MA et al.'15]

Issues with Data-Driven Reconstruction



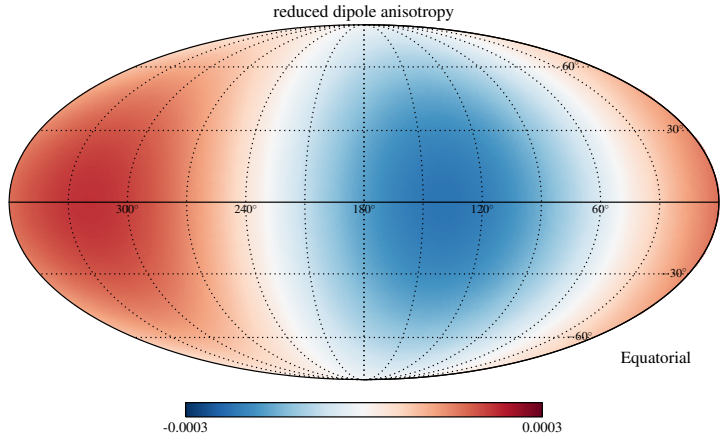
- ground-based detectors need to be **calibrated** by CR data
- true CR dipole defined by amplitude A_1 , and orientation $(\text{RA}, \text{DEC}) = (\alpha_1, \delta_1)$
- ✗ observable: projected dipole with amplitude $A'_1 = A_1 \cos \delta_1$ and orientation $(\alpha_1, 0)$
[Iuppa & Di Sciascio'13; MA et al.'15]

Issues with Data-Driven Reconstruction



- ground-based detectors need to be **calibrated** by CR data
- true CR dipole defined by amplitude A_1 , and orientation $(\text{RA}, \text{DEC}) = (\alpha_1, \delta_1)$
- ✗ observable: projected dipole with amplitude $A'_1 = A_1 \cos \delta_1$ and orientation $(\alpha_1, 0)$
[Iuppa & Di Sciascio '13; MA et al.'15]

Issues with Data-Driven Reconstruction



- ground-based detectors need to be **calibrated** by CR data
- true CR dipole defined by amplitude A_1 , and orientation $(\text{RA}, \text{DEC}) = (\alpha_1, \delta_1)$
- ✗ observable: **projected dipole** with amplitude $A'_1 = A_1 \cos \delta_1$ and orientation $(\alpha_1, 0)$
[Iuppa & Di Sciascio '13; MA et al.'15]

Large-Scale Anisotropy

Cosmic Ray Dipole Anisotropy

- Spherical harmonics expansion of relative intensity yields:

$$I(\Omega) = 1 + \underbrace{\delta \cdot \hat{n}(\Omega)}_{\text{dipole}} + \sum_{\ell \geq 2} \sum_m a_{\ell m} Y^{\ell m}(\Omega)$$

- cosmic ray density $n_{\text{CR}} \propto E^{-\Gamma_{\text{CR}}}$ and dipole vector δ from **diffusion theory**:

$$\underbrace{\partial_t n_{\text{CR}} \simeq \nabla \cdot (\mathbf{K} \nabla n_{\text{CR}}) + Q_{\text{CR}}}_{\text{diffusion equation}} \quad \text{and} \quad \underbrace{\delta \simeq 3 \mathbf{K} \nabla n_{\text{CR}} / n_{\text{CR}}}_{\text{from Fick's law}}$$

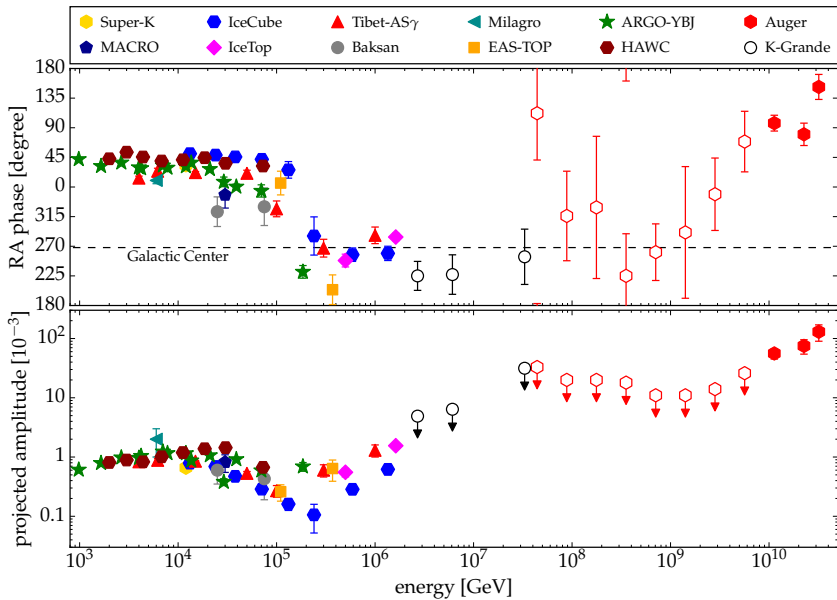
- diffusion tensor \mathbf{K} in general anisotropic (background field \mathbf{B}):

$$K_{ij} = \kappa_{\parallel} \widehat{B}_i \widehat{B}_j + \kappa_{\perp} (\delta_{ij} - \widehat{B}_i \widehat{B}_j) + \kappa_A \epsilon_{ijk} \widehat{B}_k$$

- relative motion v** of the observer in plasma rest frame (\star): [Compton & Getting'35]

$$\delta = \delta^* + \underbrace{(2 + \Gamma_{\text{CR}}) v / c}_{\text{Compton-Getting effect}}$$

Cosmic Ray Dipole Anisotropy



TeV-PeV Dipole Anisotropy

- reconstructed diffuse dipole:

$$\delta^* = \delta - \underbrace{(2 + \Gamma_{\text{CR}})\beta}_{\text{Compton-Getting}} = 3\mathbf{K} \cdot \nabla n^* / n^*$$

- projection onto equatorial plane: 

$$\delta_{\text{EP}}^* = (\delta_{0h}^*, \delta_{6h}^*)$$

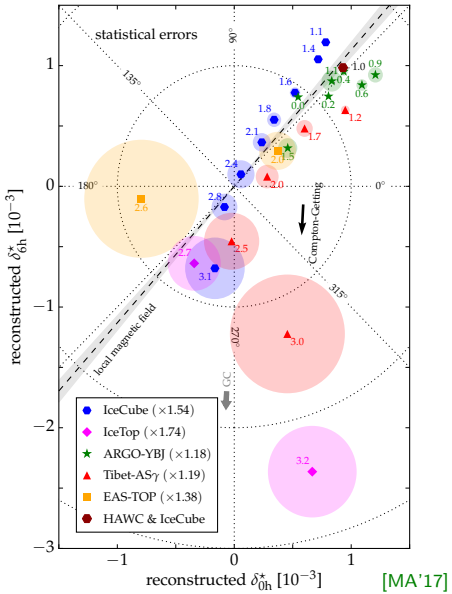
- strong regular magnetic fields** in the local environment

→ diffusion tensor reduces to **projector**:

[e.g. Mertsch & Funk'14; Schwadron et al.'14]

$$K_{ij} \rightarrow \kappa_{\parallel} \hat{B}_i \hat{B}_j$$

- TeV–PeV dipole data is consistent with magnetic field direction inferred by IBEX data.
[McComas et al.'09]

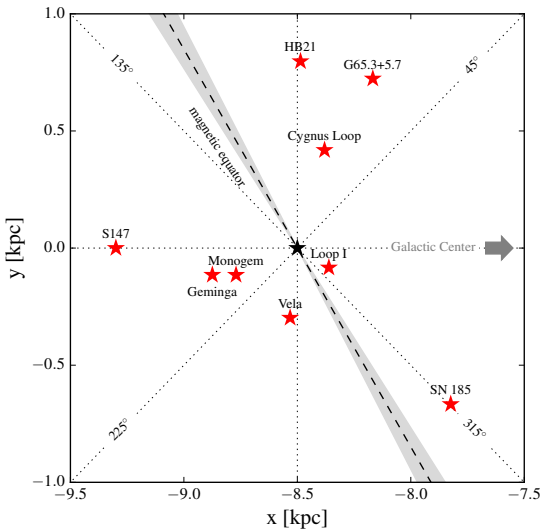


Known Local Supernova Remnants

- projection maps source gradient onto $\hat{\mathbf{B}}$ or $-\hat{\mathbf{B}}$
- **dipole phase** α_1 depends on orientation of magnetic hemispheres
- intersection of magnetic equator with Galactic plane defines two source groups:

$$120^\circ \lesssim l \lesssim 300^\circ \rightarrow \alpha_1 \simeq 49^\circ$$

$$-60^\circ \lesssim l \lesssim 120^\circ \rightarrow \alpha_1 \simeq 229^\circ$$



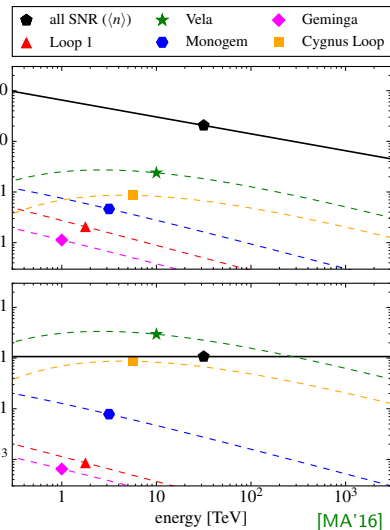
Phase-Flip by Vela SNR?

- 1–100 TeV phase indicates dominance of a local source within longitudes:

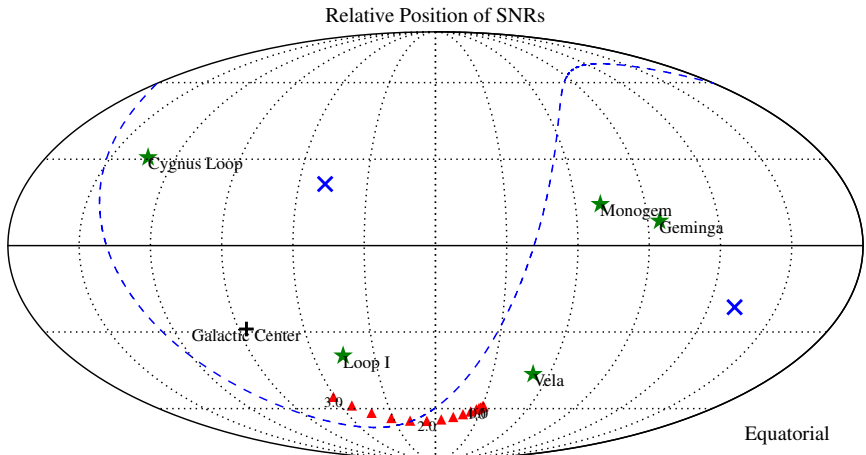
$$120^\circ \lesssim l \lesssim 300^\circ$$

- plausible scenario: Vela SNR [MA'16]

- age : $\simeq 11,000$ yrs
- distance : $\simeq 1,000$ lyrs
- SNR rate : $\mathcal{R}_{\text{SNR}} = 1/30 \text{ yr}^{-1}$
- (effective) isotropic diffusion:
$$K_{\text{iso}} \simeq 4 \times 10^{28} (E/3\text{GeV})^{1/3} \text{cm}^2/\text{s}$$
- Galactic half height : $H \simeq 3$ kpc
- instantaneous CR emission (Q_*)



Position of Local SNR



Relative position of the five closest known SNRs. The magnetic field direction (IBEX) is indicated by blue **x** and the **magnetic horizon** by a dashed line.

Phase-Flip by Vela SNR

- 1–100 TeV phase indicates dominance of a local source within longitudes:

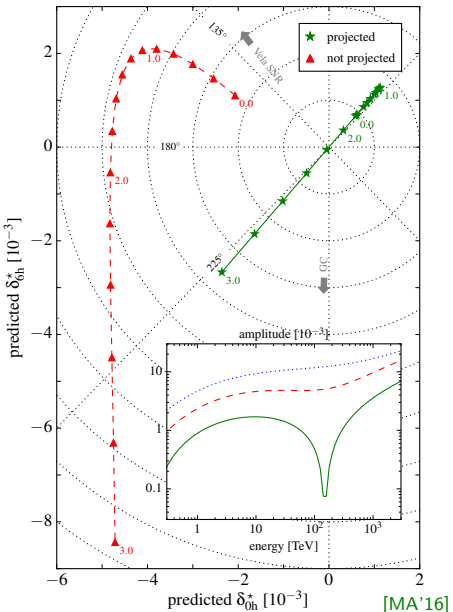
$$120^\circ \lesssim l \lesssim 300^\circ$$

- plausible scenario: Vela SNR [MA'16]

- age : $\simeq 11,000$ yrs
- distance : $\simeq 1,000$ lyrs
- SNR rate : $\mathcal{R}_{\text{SNR}} = 1/30 \text{ yr}^{-1}$
- (effective) isotropic diffusion:

$$K_{\text{iso}} \simeq 4 \times 10^{28} (E/3\text{GeV})^{1/3} \text{cm}^2/\text{s}$$

- Galactic half height : $H \simeq 3$ kpc
- instantaneous CR emission (Q_\star)

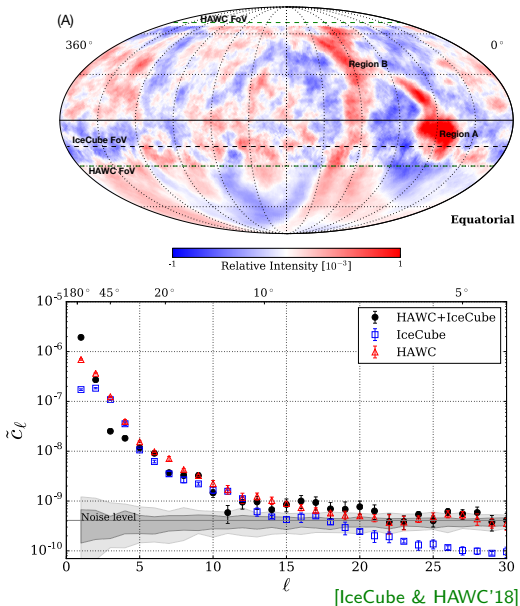


Small-Scale Anisotropy

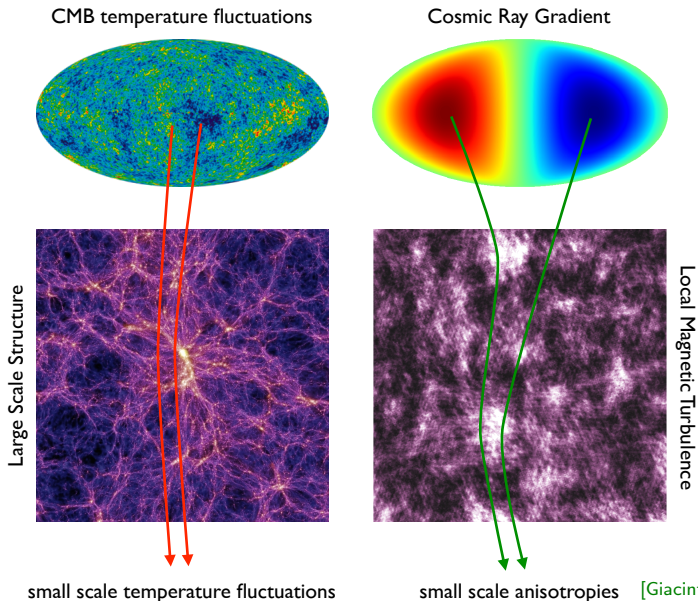
Small-Scale Anisotropy

- Significant TeV small-scale anisotropies down to angular scales of $\mathcal{O}(10)$ degrees.
- Strong local excess (“region A”) observed by Northern observatories.
[Tibet-AS γ '06; Milagro'08]
[ARGO-YBJ'13; HAWC'14]
- Angular power spectra of IceCube and HAWC data show excess compared to isotropic arrival directions. [IceCube'11; HAWC'14]

$$C_\ell = \frac{1}{2\ell+1} \sum_{m=-\ell}^{\ell} |a_{\ell m}|^2$$



Small-Scale Anisotropy from Local Turbulence



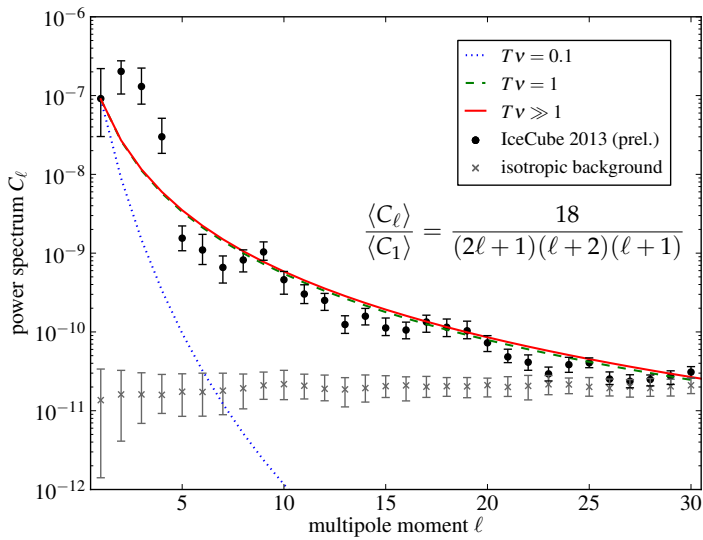
Small-Scale “Theorem”

- *Assumptions:*
 - absences of cosmic ray sources and sinks
 - isotropic and static magnetic turbulence
 - initially, homogeneous phase space distribution
- *Theorem:* The sum over the ensemble-averaged angular power spectrum is constant:

$$\sum_{\ell} (2\ell + 1) \langle C_{\ell}(t) \rangle = \text{const}$$

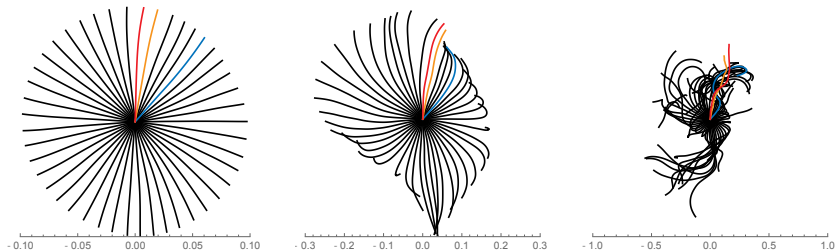
- Proof via **Liouville's theorem and angular auto-correlation function.** [MA'14]
- Wash-out of individual moments by diffusion (rate $\nu_{\ell} \propto \ell(\ell + 1)$) has to be compensated by **generation of small-scale anisotropy**.
- Theorem implies small-scale angular features from large-scale average dipole anisotropy. [Giacinti & Sigl'12; MA'14; MA & Mertsch'15]

Comparison to CR Data



[MA'14]

Simulation via Backtracking



- Consider a local (quasi-)stationary solution of the **diffusion approximation**:

$$4\pi \langle f \rangle \simeq n_{\text{CR}} + \underbrace{(\mathbf{r} - 3\hat{\mathbf{p}}\mathbf{K})\nabla n_{\text{CR}}}_{\text{1st order correction}}$$

- Ensemble-averaged C_ℓ 's ($\ell \geq 1$):

[MA & Mertsch'15]

$$\frac{\langle C_\ell \rangle}{4\pi} \simeq \int \frac{d\hat{\mathbf{p}}_1}{4\pi} \int \frac{d\hat{\mathbf{p}}_2}{4\pi} P_\ell(\hat{\mathbf{p}}_1 \hat{\mathbf{p}}_2) \lim_{T \rightarrow \infty} \underbrace{\langle \mathbf{r}_{1i}(-T) \mathbf{r}_{2j}(-T) \rangle}_{\text{relative diffusion}} \frac{\partial_i n_{\text{CR}} \partial_j n_{\text{CR}}}{n_{\text{CR}}^2}$$

Simulation via Backtracking

- simulation in isotropic & static magnetic turbulence with

$$\overline{\delta \mathbf{B}^2} = \mathbf{B}_0^2$$

- relative orientation of CR gradient:

- solid lines : $\mathbf{B}_0 \parallel \nabla n$
- dotted lines : $\mathbf{B}_0 \perp \nabla n$

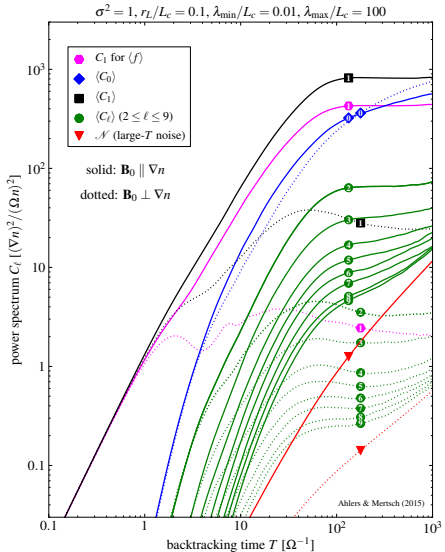
- diffusive regime at $T\Omega \gtrsim 100$

- enhanced dipole predictions:*

$$\langle C_1 \rangle > \textcolor{magenta}{C_1 \text{ for } \langle f \rangle}$$

- asymptotically **limited by simulation noise**:

$$\mathcal{N} \simeq \frac{4\pi}{N_{\text{pix}}} 2 T K_{ij}^s \frac{\partial_i n \partial_j n}{n^2}$$



[MA & Mertsch'15]

Summary and Outlook

- Observation of CR anisotropies at the level of **one-per-mille** is challenging.
 - Reconstruction methods can **introduce bias**, sometimes not stated or corrected for.
 - **Dipole anisotropy** can be understood in the context of standard diffusion theory:
 - TeV-PeV dipole phase aligns with local ordered magnetic field.
 - Amplitude variations as a result of local sources
 - Plausible & natural candidate: **the Vela supernova remnant**
 - Observed CR data shows evidence of **small-scale anisotropy**.
 - Influenced by heliosphere?
 - Effect from non-uniform pitch-angle diffusion?
 - Result of local magnetic turbulence?
- ✓ Both observations allow to **probe our local magnetic environment**.
- Future **TeV–EeV CR data** (e.g. from LHAASO) with improved energy resolution and event statistics will allow to decipher large- and small-scale features in presently uncharted territory.
- Joint analyses of data from Northern and Southern observatories (e.g. from SWGO & IceCube-Gen2) benefit from **extended FoV** and reduced multipole cross-talk.

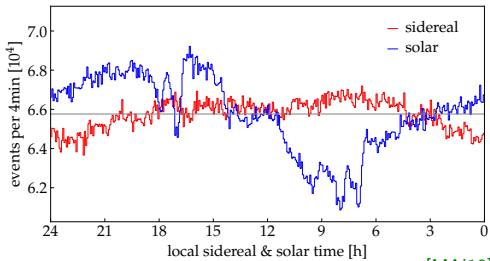
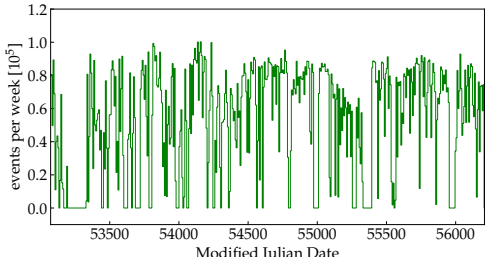
Appendix

KASCADE-Grande Data

- KASCADE-Grande in Karlsruhe, Germany (49.1° N, 8.4° E)
- data collected between March 2004 and October 2012
- available via: kcdc.ikp.kit.edu
- three energy bins from N_{ch} cuts:

data	E_{med}^*	N_{ch} -range	N_{tot}
sidereal	–	$\geq 10^{5.2}$	23,674,844
solar	–	$[10^{5.2}, 10^{5.6})$	17,443,774
bin 1	2.7 PeV	$[10^{5.2}, 10^{5.6})$	17,443,774
bin 2	6.1 PeV	$[10^{5.6}, 10^{6.4})$	6,084,275
bin 3	33 PeV	$\geq 10^{6.4}$	146,795

- Full anisotropy construction in Northern Hemisphere possible with max- \mathcal{L} method. [MA'19]

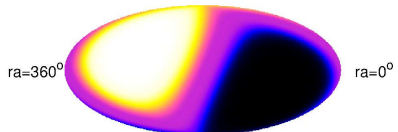


[MA'19]

Non-Uniform Pitch-Angle Diffusion

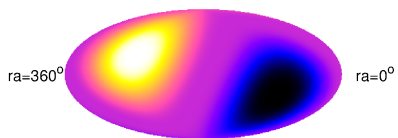
- stationary pitch-angle diffusion ($\mu \equiv \cos \theta$) :

$$v\mu \frac{\partial}{\partial z} \langle f \rangle = \frac{\partial}{\partial \mu} D_{\mu\mu} \frac{\partial}{\partial \mu} \langle f \rangle$$

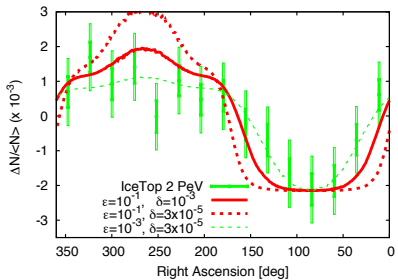


- non-uniform** diffusion:

$$\frac{D_{\mu\mu}}{1 - \mu^2} \neq \text{const}$$

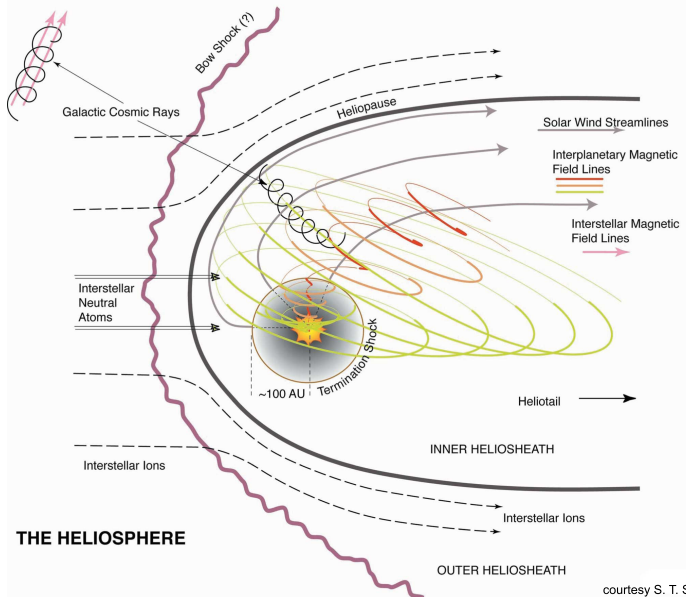


- non-uniform pitch-angle diffusion modifies the large-scale anisotropy aligned with \mathbf{B}_0
 - small scale excess/deficits** for enhanced diffusion towards $\mu \simeq \pm 1$
[Malkov, Diamond, Drury & Sagdeev'10]
 - modified large-scale features** for enhanced diffusion at $\mu \simeq 0$
[Giacinti & Kirk'17]



[Giacinti & Kirk'17]

Small-Scale Anisotropies from Heliosphere?



courtesy S. T. Suess

Small-Scale Anisotropies from Heliosphere?

- **Solar potential** affects cosmic ray flux (monopole) only at rigidity $\mathcal{R} \lesssim \text{GV}$.
[Gleeson & Axford'68; Gleeson & Urch'73]

- However, gyroradius of sub-TV cosmic rays smaller than the size of heliosphere:

$$r_g \simeq 200 \left(\frac{\mathcal{R}}{\text{TV}} \right) \left(\frac{B}{\mu\text{G}} \right)^{-1} \text{AU}$$

- various effects and studies:

- ★ hard CR spectra via magnetic reconnection in the heliotail [Lazarian & Desiati'10]
- ★ non-isotropic particle transport in the heliosheath [Desiati & Lazarian'11]
- ★ heliospheric electric fields induced by plasma motion [Drury'13]
- ★ simulation via CR back-tracking in MHD simulation of heliosphere
[Zhang, Zuo & Pogorelov'14; López-Barquero et al.'16]

Solar Potential

- dipole anisotropy induced by CR diffusion in solar wind:

$$|\Phi| = - \underbrace{\frac{\beta_{\odot}(r)}{3} \frac{\partial \phi}{\partial \ln p}}_{\text{Compton-Getting}} - \underbrace{\kappa_{\odot}(r, p) \frac{\partial \phi}{\partial r}}_{\text{diffuse dipole}}$$

→ **force-field approximation:** $|\Phi| \simeq 0$ [Gleeson & Axford'68; Gleeson & Urch'73]

- local solution related to distribution beyond heliosphere:

$$\phi(r_{\oplus}, p(r_{\oplus})) = \lim_{R \rightarrow \infty} \phi(R, p(R))$$

- $p(r)$ solution of **characteristic equation**:

$$\frac{\partial p}{\partial r} = \frac{\beta_{\odot}(r)}{3} \frac{p}{\kappa_r(r, p)}$$

→ assume **Bohm diffusion** in heliosphere: $\kappa_{\odot}(r, p) \simeq \kappa_0(r)(\mathcal{R}/\mathcal{R}_0)$

$$p(r_{\oplus}) = p(\infty) - |Z|eV_{\odot} \quad \text{with} \quad V_{\odot} = \underbrace{\frac{\mathcal{R}_0}{3} \int_{r_{\oplus}}^{\infty} dr' \frac{\beta_{\odot}(r')}{\kappa_0(r')}}_{\text{effective "solar potential"}} \lesssim 1 \text{ GV}$$

Simulated Turbulence

- 3D-isotropic turbulence:

[Giacalone & Jokipii'99]

$$\delta \mathbf{B}(\mathbf{x}) = \sum_{n=1}^N A(k_n) (\mathbf{a}_n \cos \alpha_n + \mathbf{b}_n \sin \alpha_n) \cos(\mathbf{k}_n \cdot \mathbf{x} + \beta_n)$$

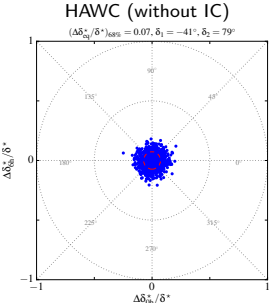
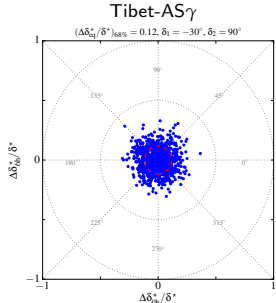
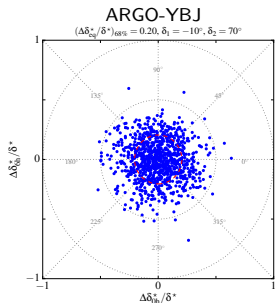
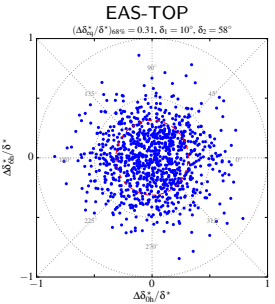
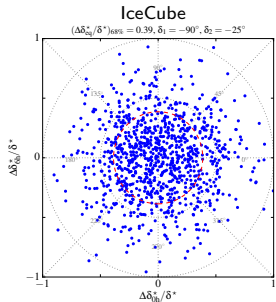
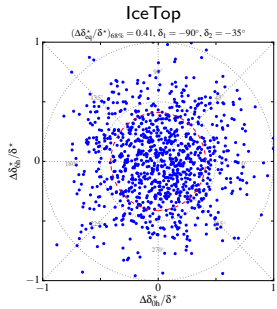
- α_n and β_n are random phases in $[0, 2\pi)$, unit vectors $\mathbf{a}_n \propto \mathbf{k}_n \times \mathbf{e}_z$ and $\mathbf{b}_n \propto \mathbf{k}_n \times \mathbf{a}_n$
- with amplitude

$$A^2(k_n) = \frac{2\sigma^2 B_0^2 G(k_n)}{\sum_{n=1}^N G(k_n)} \quad \text{with} \quad G(k_n) = 4\pi k_n^2 \frac{k_n \Delta \ln k}{1 + (k_n L_c)^\gamma}$$

- Kolmogorov-type turbulence: $\gamma = 11/3$
- $N = 160$ wavevectors \mathbf{k}_n with $|\mathbf{k}_n| = k_{\min} e^{(n-1)\Delta \ln k}$ and $\Delta \ln k = \ln(k_{\max}/k_{\min})/N$
- $\lambda_{\min} = 0.01L_c$ and $\lambda_{\max} = 100L_c$
- rigidity: $r_L = 0.1L_c$
- turbulence level: $\sigma^2 = \mathbf{B}_0^2 / \langle \delta \mathbf{B}^2 \rangle = 1$

[Fraschetti & Giacalone'12]

Systematic Uncertainty of CR Dipole



Compton-Getting Effect

- phase-space distribution is **Lorentz-invariant**

$$f(\mathbf{p}) = f^*(\mathbf{p}^*)$$

- relative motion of observer ($\beta = \mathbf{v}/c$) in plasma rest frame (*):

$$\mathbf{p}^* = \mathbf{p} + p\beta + \mathcal{O}(\beta^2)$$

- Taylor expansion:

$$f(\mathbf{p}) \simeq f^*(\mathbf{p}) + (\mathbf{p}^* - \mathbf{p}) \nabla_{\mathbf{p}^*} f^*(\mathbf{p}) + \mathcal{O}(\beta^2) \simeq f^*(\mathbf{p}) + p\beta \nabla_{\mathbf{p}^*} f^*(\mathbf{p}) + \mathcal{O}(\beta^2)$$

→ dipole term Φ is **not invariant**:

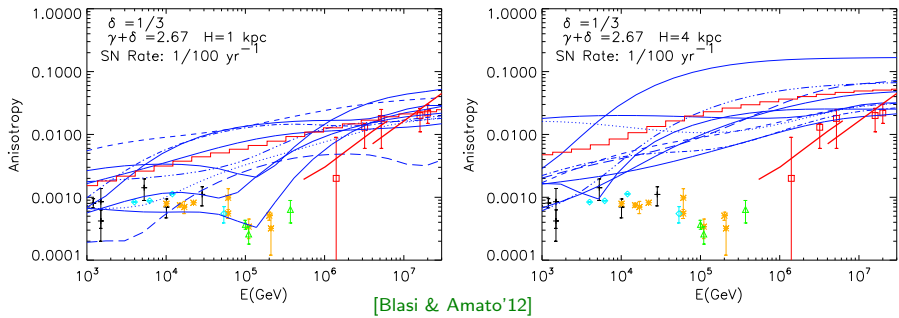
$$\phi = \phi^* \quad \text{and} \quad \Phi = \Phi^* + \frac{1}{3}\beta \frac{\partial \phi^*}{\partial \ln p}$$

- with $\phi \sim p^{-2} n_{\text{CR}} \propto p^{-2-\Gamma_{\text{CR}}}$:

$$\delta = \delta^* + \underbrace{(2 + \Gamma_{\text{CR}})\beta}_{\text{Compton-Getting effect}}$$

✗ What is the plasma rest-frame? LSR or ISM : $v \simeq 20 \text{ km/s}$

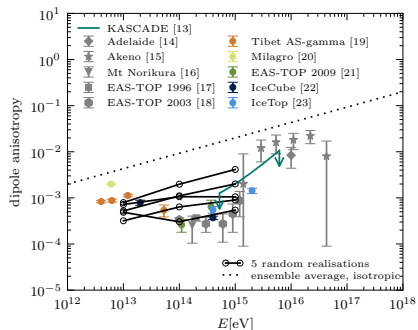
Local Sources



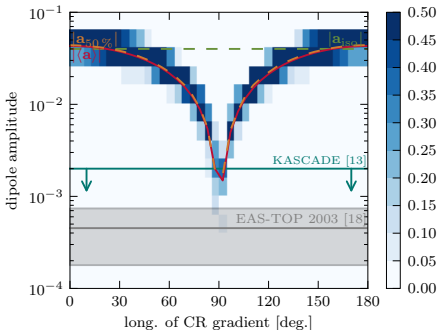
- Distribution of local cosmic ray sources (SNR) in position and time induces variation in the anisotropy.
[Erlykin & Wolfendale'06; Blasi & Amato'12]
[Sveshnikova et al.'13; Pohl & Eichler'13]
- variance of amplitude can be estimated as:
[Blasi & Amato'12]

$$\sigma_A \propto \frac{K(E)}{cH} \quad \rightarrow \quad \frac{\sigma_A}{A} = \text{const}$$

Local Magnetic Field



[Mertsch & Funk'14]



- **strong regular magnetic fields** in the local environment
- diffusion tensor reduces to **projector**: [e.g. Mertsch & Funk'14; Schwadron *et al.*'14; MA'17]

$$K_{ij} \rightarrow \kappa_{\parallel} \hat{B}_i \hat{B}_j$$

- **reduced dipole amplitude and alignment with magnetic field:** $\delta \parallel \mathbf{B}$

Local Magnetic Field

- **IBEX ribbon:** enhanced emission of energetic neutral atoms (ENAs) observed with Interstellar Boundary EXplorer [McComas et al.'09]

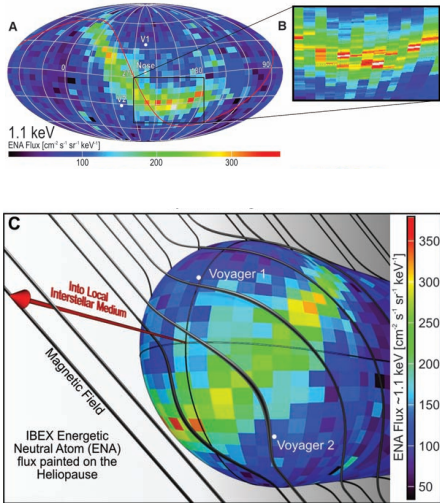
- interpreted as local magnetic field ($\lesssim 0.1$ pc) drapping the heliosphere
- circle center defines field orientation (in Galactic coordinate system):

[Funsten et al.'13]

$$l \simeq 210.5^\circ \quad \& \quad b \simeq -57.1^\circ \\ (\Delta\theta \simeq 1.5^\circ)$$

- consistent with starlight polarization by interstellar dust ($\lesssim 40$ pc) [Frisch et al.'15]

$$l \simeq 216.2^\circ \quad \& \quad b \simeq -49.0^\circ$$



[McComas et al.'09]

Evolution Model

- Diffusion theory motivates that each $\langle C_\ell \rangle$ decays exponentially with an effective **relaxation rate** [Yosida'49]

$$\nu_\ell \propto L^2 \propto \ell(\ell+1)$$

- A **linear** $\langle C_\ell \rangle$ evolution equation with generation rates $\nu_{\ell \rightarrow \ell'}$ requires:

$$\partial_t \langle C_\ell \rangle = -\nu_\ell \langle C_\ell \rangle + \sum_{\ell' \geq 0} \nu_{\ell' \rightarrow \ell} \frac{2\ell' + 1}{2\ell + 1} \langle C_{\ell'} \rangle \quad \text{with} \quad \nu_\ell = \sum_{\ell' \geq 0} \nu_{\ell \rightarrow \ell'}$$

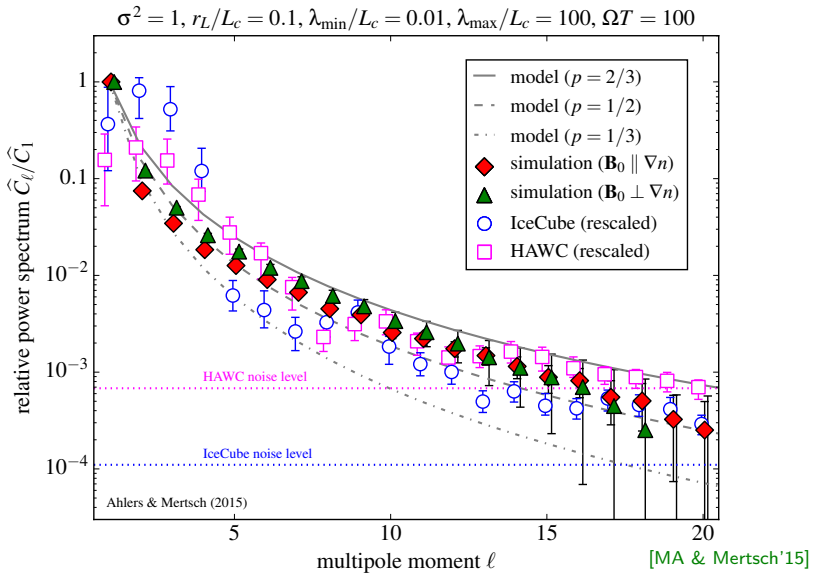
- For $\nu_\ell \simeq \nu_{\ell \rightarrow \ell+1}$ and $\tilde{C}_\ell = 0$ for $\ell \geq 2$ this has the analytic solution:

$$\langle C_\ell \rangle(T) \simeq \frac{3\tilde{C}_1}{2\ell + 1} \prod_{m=1}^{\ell-1} \nu_m \sum_n \prod_{p=1 (\neq n)}^{\ell} \frac{e^{-T\nu_p}}{\nu_p - \nu_n}$$

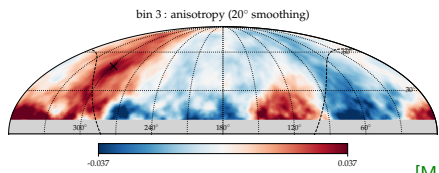
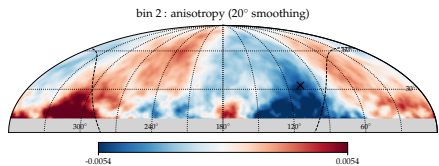
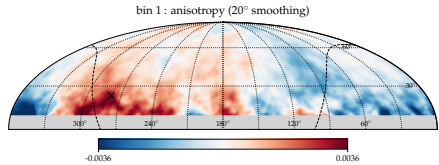
- For $\nu_\ell \simeq \ell(\ell+1)\nu$ we arrive at a **finite asymptotic ratio**:

$$\lim_{T \rightarrow \infty} \frac{\langle C_\ell \rangle(T)}{\langle C_1 \rangle(T)} \simeq \frac{18}{(2\ell+1)(\ell+2)(\ell+1)}$$

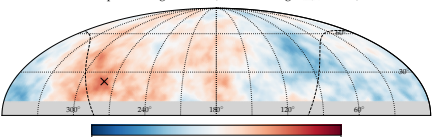
Simulation vs. Data



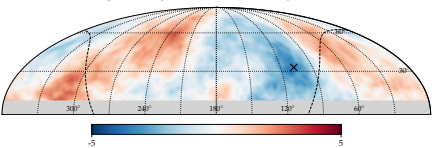
Example: KASCADE-Grande



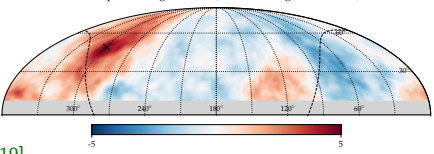
bin 1 : pre-trial significance (20° smoothing, $\sigma_{\max} = 3.09$)



bin 2 : pre-trial significance (20° smoothing, $\sigma_{\max} = 3.54$)



bin 3 : pre-trial significance (20° smoothing, $\sigma_{\max} = 4.73$)

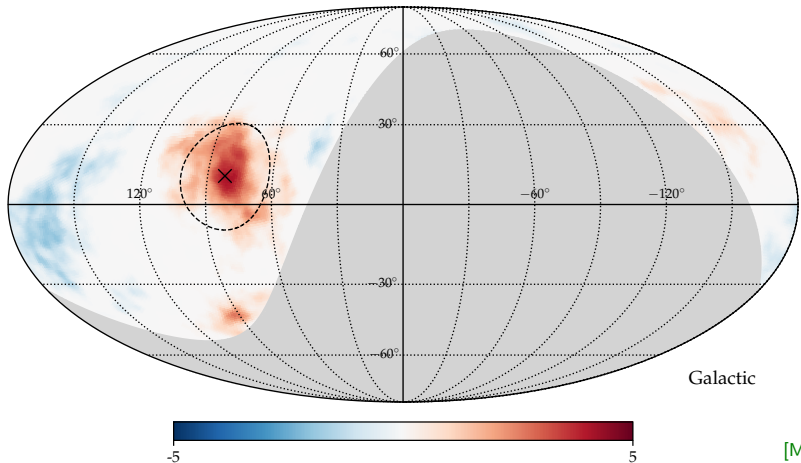


[MA'19]

Sidereal anisotropy in the KASCADE-Grande data with median energy of 2.7 PeV (bin 1), 6.1 PeV (bin 2) and 33 PeV (bin 3).

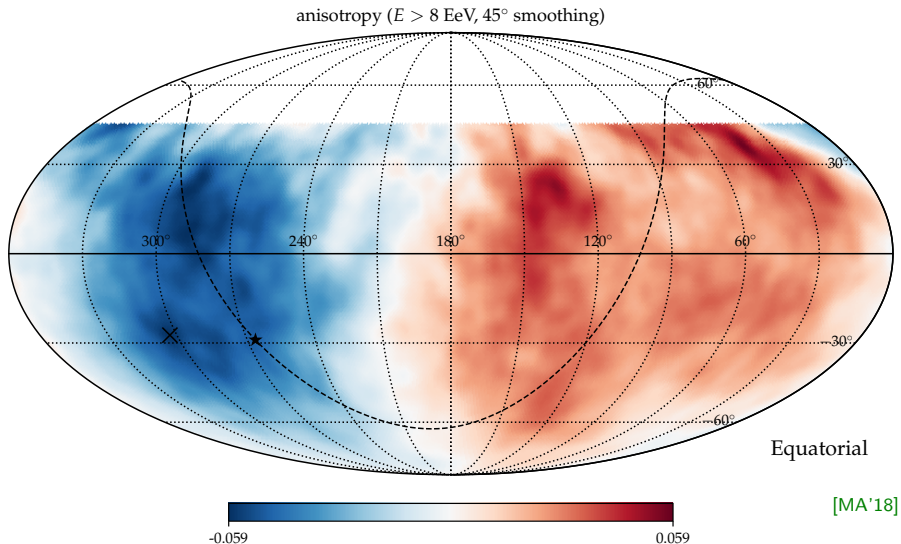
Small-Scale Feature At the 2nd Knee?

bin 3 : post-trial significance (20° smoothing, $\sigma_{\max} = 4.16$)



Small-scale anisotropy of 33 PeV cosmic rays overlaps with Cygnus region.
(gyro radius < 10 pc; neutron decay length $\simeq 300$ pc)

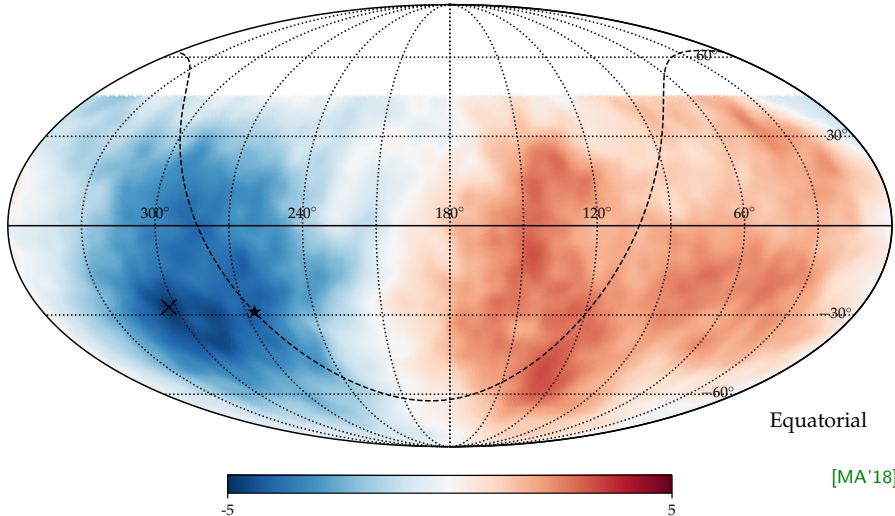
Example: Pierre Auger



Method can also be applied to high-energy data beyond the knee, e.g. Auger.

Example: Pierre Auger

pre-trial significance ($E > 8 \text{ EeV}$, 45° smoothing, $\sigma_{\max} = 4.86$)



Method can also be applied to high-energy data beyond the knee, e.g. Auger.